Lateral–torsional buckling resistance of coped beams

J. Maljaars[a,b,*], J.W.B. Stark[c], H.M.G.M. Steenbergen[b],
R. Abspoel[c]

[a]*Eindhoven University of Technology, Faculty of Architecture, Building and Planning, P.O. Box 513,
5600 MB Eindhoven, The Netherlands*
[b]*TNO Built Environment and Geosciences, P.O. Box 49, 2600 AA Delft, The Netherlands*
[c]*Delft University of Technology, Faculty of Civil Engineering and Geosciences, P.O. Box 5048, 2600 GA Delft,
The Netherlands*

Abstract

The lateral–torsional buckling resistance of beams depends on the support conditions. In floor structures for buildings coped beams are often used. A numerical model was developed to investigate the influence of copes on the lateral buckling resistance. This model is described in a companion paper [Maljaars J, Stark JWB, Steenbergen HMGM, Abspoel R. Development and validation of a numerical model for buckling of coped beams. Journal of Constructional Steel Research 2005;61(11):1576–93]. In this paper results of a parameter study carried out with the numerical model are presented. Based on these results recommendations for design rules are given. The study is restricted to (coped) beams with end plates.
© 2005 Elsevier Ltd. All rights reserved.

Keywords: Lateral–torsional buckling; Design of buildings; Cope; Endplate; Connection

1. Introduction

The well-known equation for the elastic critical buckling load for lateral–torsional buckling (M_{cr}) of a beam loaded with a uniform bending moment was published in 1960

---

* Corresponding author at: Eindhoven University of Technology, Faculty of Architecture, Building and Planning, P.O. Box 513, 5600 MB Eindhoven, The Netherlands. Tel.: +31 15 2763464.
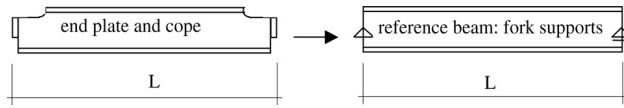*E-mail address:* johan.maljaars@tno.nl (J. Maljaars).

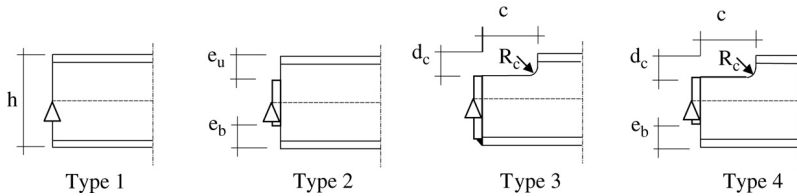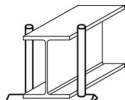Fig. 1. Comparison between coped beam and beam with fork supports.

Fig. 2. Studied connections.

by Timoshenko and Gere (Eq. (1)). The equation was analytically derived for a simply supported beam with fork supports, i.e. the rotation about the longitudinal axis and vertical and lateral deflections are restrained, while rotations about the strong and weak axes are free. In addition, the beam ends are assumed free to warp, but no other distortion of the beam end is allowed.

$$M_{cr} = \frac{\pi}{L} \sqrt{E I_z \left(G I_t + \frac{\pi^2}{L^2} E I_{wa} \right)} \qquad (1)$$

Conditions for fork supports are not always fulfilled in connections applied in practice. When copes are used, local web deformation in the coped part or lateral–torsional buckling of the coped part of the section may reduce the elastic critical buckling load of the entire section [4,3]. Local web deformation may also occur if endplates are not welded to the full height of the section end.

In order to quantify the influence of copes and partial end plates on the elastic critical buckling load and on the buckling resistance, a parameter study was carried out with the numerical models, described in [1].

Buckling of coped beams of various sizes supported by two types of end plates and with various dimensions of copes were compared with buckling of a reference beam with equal properties, but with a uniform cross-section and with fork supports, see Fig. 1.

The influence of the support conditions on the elastic critical buckling load is expressed by a reduction factor on the elastic critical buckling load of the reference beam (Eq. (1)). The equations for these reduction factors were based on curve fitting of the numerically obtained results. For the determination of the ultimate buckling resistance from the elastic critical buckling load, appropriate buckling curves are proposed.

2. Parameter field

Four different types of end condition as shown in Fig. 2 were considered:

1. Beam with uniform cross-section and fork supports. This is the reference beam;
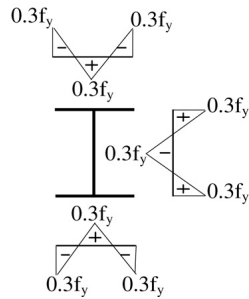2. Beam with uniform cross-section and end plates;

Fig. 3. Residual stresses in NEN 6771 [12].

3. Coped beam with endplates welded to the bottom flange (long end plates);
4. Coped beam with endplates welded to a part of the web only (short end plates).

The beams were simply supported on the outside of the endplate at mid-height of the full section as shown in Fig. 2.

The following parameters were varied (symbols are explained in Figs. 1 and 2):

1. Section size: IPE160, IPE330 and IPE500;
2. Slenderness: $7 < h/L < 40$;
3. Distance from upper side of the endplate to the top of the beam e_u: $0 < e_u <$ min (65 mm, $1/4h$);
4. Distance from underside of the endplate to the bottom of the beam e_b: $0 < e_b <$ min (65 mm, $1/4h$);
5. Cope length c: 40 mm $< c <$ 230 mm;
6. Cope depth d_c: $0 < d_c <$ min ($1/4h$, 65 mm);
7. Load cases: uniformly distributed load applied in the center of the upper flange or in the section centroid.

According to numerical simulations, the cope radius R_c has no significant influence on the ultimate resistance and was therefore not varied. R_c was set equal to the radius of the section root.

According to previous research [1–9], the influence of the cope increases with increasing depth to span ratio. Therefore, most calculations were carried out on relatively stocky beams.

The material strength was not varied, but taken according to S235. The entire stress–strain relation of S235, including strain hardening, was applied.

Residual stresses and geometrical imperfections may influence the ultimate buckling resistance. In the numerical simulations residual stresses with a pattern according to Fig. 3 were applied. This pattern is given in the Dutch code for steel structures, NEN 6771 [12].

Initial geometric imperfections were modelled by scaling the first elastic critical buckling mode with an amplitude of 0.1% of the span ($A = 0.001L$). As the second eigenvalue is approximately two times higher than the first eigenvalue, the deformed shape of a real beam will be dominated by the first elastic critical buckling mode. Applying
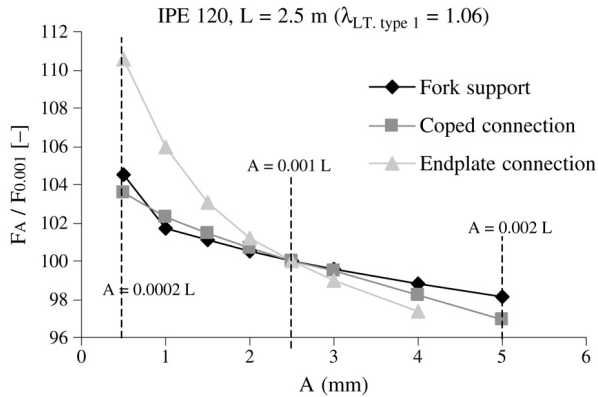
Fig. 4. Influence of amplitude of initial geometric imperfection (A) on resistance.

imperfections by scaling the first mode, the simulations will give a conservative buckling resistance. This method has been used also by others, e.g. by Greiner et al. [10].

In order to check the influence of the amplitude on the resistance, a sensitivity analysis was carried out for the following three cases:

- The reference beam (type 1).
- A beam of uniform cross-section with short end plates (type 2).
- A coped beam with long end plates (type 3).

  Data:

- Beam size: IPE120.
- Loading: concentrated load at midspan, applied in the center of the upper flange.
- Span: 2.5 m. It is expected that for this span the influence of initial imperfections is relatively large.

Results are shown in Fig. 4, where the calculated resistances are normalized to the resistance $F_{0.001}$ of a beam with amplitude $A = 0.001L$.

The resistance increases up to 10% if the nominal imperfection is $1/5000L$ instead of $1/1000L$. Larger imperfections than $1/1000L$ do not result in significant smaller resistances. When real beam imperfections are not known, an imperfection of $1/1000L$ seems to be a realistic assumption. Moreover, the calculations are compared to the buckling curves in EN1993-1-1 [11]. These buckling curves are partially based on the results by Greiner. It is therefore appropriate to apply the same imperfection as applied by Greiner.

Beams with short end plates and coped beams are more sensitive to variation of the initial imperfection than the reference beam.

3. Influence of connections on the elastic critical buckling load

The influence of connections on the elastic critical buckling load is expressed by a reduction factor α. This factor is defined as the ratio between the elastic critical buckling load of the beam with copes and/or endplates, and the elastic critical buckling load of the
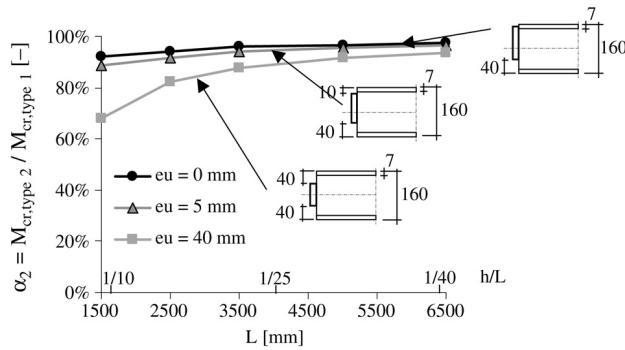
Fig. 5. Elastic critical buckling load for three end plate heights.

reference beam with fork supports and equal dimensions (Eq. (2)).

$$\alpha_{2,3\,or\,4} = \frac{M_{cr,type\,2,\,3\,or\,4}}{M_{cr,type\,1}}. \tag{2}$$

In the following sub-sections, the influence of type 2–4 connections on the elastic critical buckling load is briefly discussed. The entire parameter study, on which these results are based, is documented in Maljaars [13].

3.1. Beams of uniform cross-section with short end plates (type 2)

In Fig. 5 the numerically determined values of α_2 of IPE160 beams with endplate connections and with uniform cross-sections (type 2) are given as a function of the beam span. Lines are given for three end plate heights as indicated in the figure. The influence of the end plate height is larger for smaller spans. The maximum reduction of the elastic critical buckling load in the given range is 32% for short spans to 10% for normal spans ($h/L = 1/40$).

In Fig. 6 the values of α_2 of a stocky IPE500 beam with a depth to span ratio $h/l = 1/7$ are plotted as a function of e_u. Lines are given for three values of e_b. The relation between α_2 and e_u is approximately linear and this parameter has a significant influence on the buckling resistance of stocky beams. The lines are close together, indicating that the value of e_b in this case has a minor influence. The results of all simulations showed that the reduction due to this parameter is only significant for large values of the ratio e_b/h.

Approximately linear relations exist between α_2 and e_u or e_b. The influences of e_u or e_b decrease for decreasing depth to span ratio. This relation is non-linear. The influences of e_b and e_u are uncorrelated. Based on the numerical data Eq. (3) is proposed for α_2.

$$\alpha_2 = 1 - A_1 \cdot \frac{e_u}{h} \cdot \left(\frac{h}{L}\right)^{A_2} + A_3 \cdot \frac{e_b}{h} \cdot \left(\frac{h}{L}\right)^{A_4}. \tag{3}$$

The factors A_1 up to A_4 are:

- In the case of a distributed load applied in the center of the upper flange:
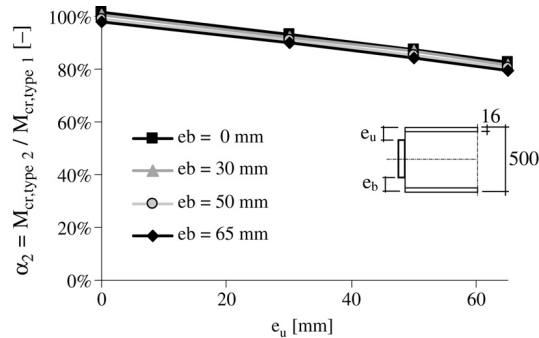 $A_1 = 22.7$; $A_2 = 1.44$; $A_3 = 0.875$; $A_4 = 0.450$.

Fig. 6. Reduction factor α_2 of beams with $h/L = 1/7$ as a function of e_u.

- In the case of a distributed load applied in the section centroid:
  $A_1 = 9.93$; $A_2 = 1.10$; $A_3 = 1.28$; $A_4 = 0.860$.

  The application is limited to standard European IPE beams (or similar sections) with:

- $160 \le h \le 500$ mm
- $L/h \ge 7.5$ but $L > 1500$ mm
- $e_u/h \le 0.25$ but $e_u \le 65$ mm
- $e_b/h \le 0.25$ but $e_b \le 65$ mm.

The maximum difference between the reduction factor determined with Eq. (3) and the reduction factor according to the numerical simulations is 2% for IPE160 and IPE330 sections and 2.6% for IPE500 sections.

3.2. Beams with copes and long end plates (type 3)

In Fig. 7 the values of α_3 of IPE160 beams are plotted against the beam span. Lines are given for six values of the cope length. The influence of copes is larger for smaller span-to-depth ratios. The maximum reduction of the elastic critical buckling load in the given range is 75% for short spans ($h/L = 1/9$) to 20% for normal spans ($h/L = 1/40$).

In Fig. 8 α_3 is given for stocky IPE160 beams ($h/L = 1/9$) with different cope lengths and cope depths. The influence of cope depth increases with decreasing cope length. The relation between α_3 and the cope depth is approximately linear.

Based on the numerical data Eqs. (4) and (5) are proposed for α_3.

$$\alpha_3 = 1 - B_1 \frac{d_c}{c} \left(\frac{h}{L}\right)^{B_2} - (B_3)^{B_4} \left(\frac{h}{L}\right)^{B_5} \tag{4}$$

$$B_3 = B_6 \left(\frac{c}{h} - B_7\right) > 0. \tag{5}$$

The factors B_1 up to B_7 are:

- For a distributed load applied in the center of the upper flange:
  $B_1 = 22.8$; $B_2 = 1.89$; $B_4 = 0.344$; $B_5 = 1.44$; $B_6 = 4457$; $B_7 = 0.229$.
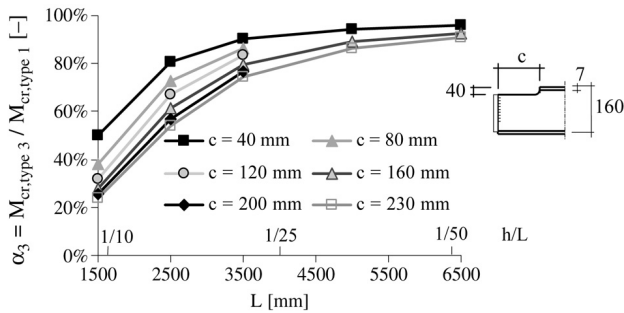
Fig. 7. Elastic critical buckling load as a function of the span for beams with type 3 connections with various cope lengths.
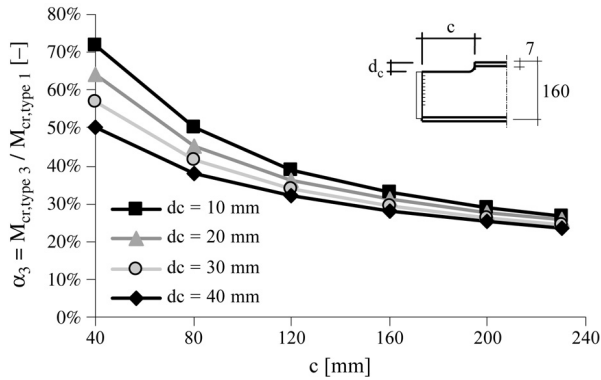

Fig. 8. Elastic critical buckling load as a function of cope length of beams with type 3 connections and $h/L = 1/9$.

- For a distributed load applied in the section centroid:
  $B_1 = 23.3$; $B_2 = 1.97$; $B_4 = 0.361$; $B_5 = 1.58$; $B_6 = 7671$; $B_7 = 0.236$.

The application is limited to standard European IPE beams (or similar sections) with:

- $160 \leq h \leq 500$ mm
- $L/h \geq 7.5$ but $L > 1500$ mm
- $c \leq 230$ mm
- $d_c \leq 40$ mm.

Lindner and Gietzelt [2] determined the elastic critical buckling load of IPE140 sections with type 3 connections, using an energy method. The cope depth d_c was 28 mm and the cope length c was 35 and 140 mm. The beams were loaded with a distributed load on the upper flange. Fig. 9 gives the comparison between their results and Eqs. (4) and (5).

The reduction of the elastic critical buckling load caused by the cope is greater according to the current research than determined by Lindner and Gietzelt.

As the current research is limited to a distributed load and the research [3,4,7] is limited to one or two concentrated loads, it is not possible to compare the results with this research.
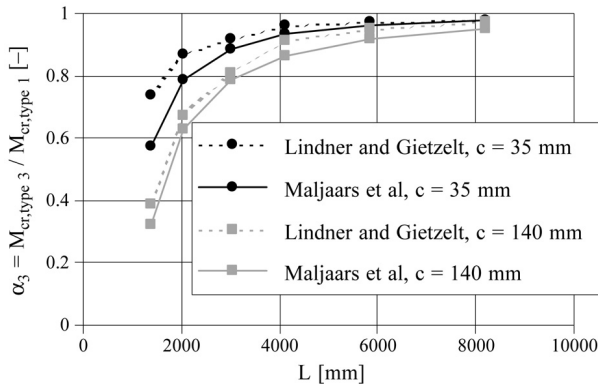
Fig. 9. Comparison of α_3 of a coped IPE140 section according to the proposed method with results of Lindner and Gietzelt [2].
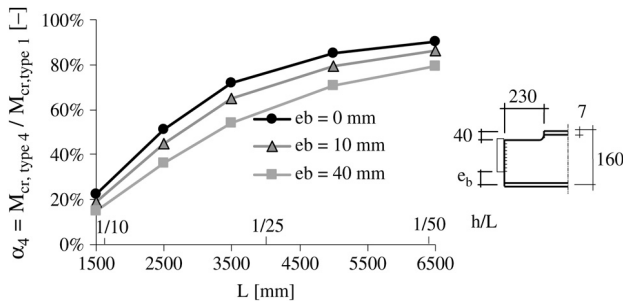

Fig. 10. Elastic critical buckling load as a function of the span for beams with type 4 connections with various values for e_b.

3.3. Beams with copes and short end plates (type 4)

Of the studied connection types, type 4 gives the worst support of the beam. It is therefore expected that beams with these connections give the largest reduction of the elastic critical buckling load. This is confirmed by the results of simulations.

In Fig. 10 values of α_4 for IPE160 beams are plotted against the beam span, for three values of e_b. The cope length of the simulations shown is 230 mm and the cope depth is 40 mm. The maximum reduction of the elastic critical buckling load in the given range is 85% for short spans ($h/L = 1/9$) to 30% for normal spans ($h/L = 1/40$).

In Fig. 11 values for α_4 are given as a function of e_b for six values of the cope length. The relation between the elastic critical buckling load and e_b is approximately linear, except for the case where the end plate covers the full web. In this case the web supplies sufficient support to the bottom flange to restrain it against rotation, although the bottom flange is not welded to the end plate (Fig. 12).

For beams without copes, the drop in the elastic critical buckling load between end plates covering the entire web and end plates covering only a part of the web was not found. The drop in elastic critical buckling load for coped beams is caused by local web
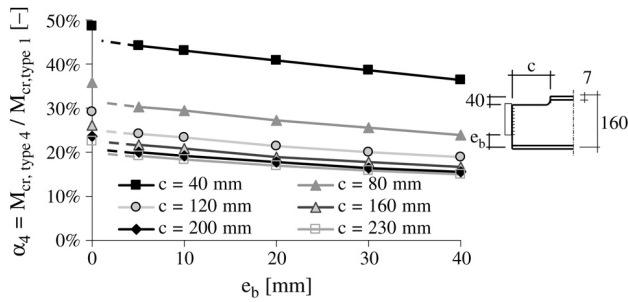
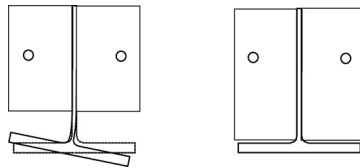Fig. 11. Elastic critical buckling load as a function of the span.

Fig. 12. Rotation of bottom flange restrained by deep end plates.

deformations, resulting in a rotation about the longitudinal axis of the web. Consequently the entire beam buckles. For this reason the influence of copes and the influence of short end plates cannot simply be combined.

Based on the numerical data Eqs. (6) and (7) are proposed for α_4.

$$\alpha_4 = 1 - D_1 \frac{d_c}{c} \left(\frac{h}{L}\right)^{D_2} - (D_3)^{D_4} \left(\frac{h}{L}\right)^{D_5} - D_8 \frac{e_b}{h} \left(\frac{h}{L}\right)^{D_9} \tag{6}$$

$$D_3 = D_6 \left(\frac{c}{h} - D_7\right) > 0. \tag{7}$$

The factors D_1 up to D_9 are:

- For a distributed load applied in the center of the upper flange:
  $D_1 = 21.5; D_2 = 1.81; D_4 = 0.288; D_5 = 1.04;$
  $D_6 = 1149; D_7 = 0.239; D_8 = 1.01; D_9 = 0.479.$
- For a distributed load applied in the section centroid:
  $D_1 = 21.6; D_2 = 1.83; D_4 = 0.322; D_5 = 1.21;$
  $D_6 = 1883; D_7 = 0.244; D_8 = 0.709; D_9 = 0.419.$

The application is limited to standard European IPE beams (or similar sections) with:

- $160 \leq h \leq 500$ mm
- $L/h \geq 7.5$ but $L > 1500$ mm
- $c \leq 230$ mm
- $d_c \leq 40$ mm
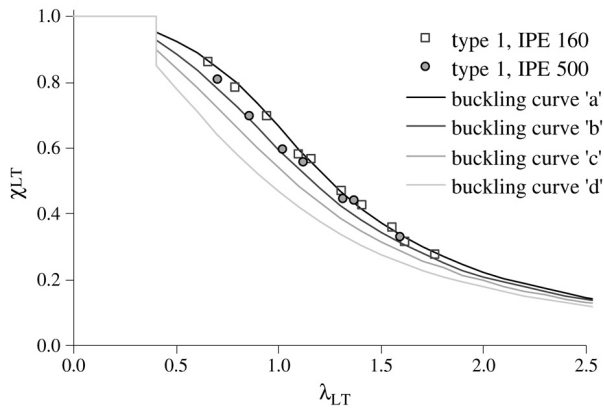- $e_b/h \leq 0.25$ but $e_b \leq 65$ mm.

Fig. 13. Buckling curves and simulations of beams with type 1 connections.

Eqs. (6) and (7) give an approximation of the real value of the elastic critical buckling load with a maximum deviation of 10%. For a more refined method it is necessary to develop an analytical model for buckling of coped beams.

4. Ultimate buckling resistance

4.1. Procedure

To determine the design resistance of a beam with type 1 connections, EN 1993-1-1 [3] provides buckling curves. By using these curves, which account for the influence of yielding, geometrical imperfections and residual stresses are taken into account. These buckling curves give the relation between the relative slenderness λ_{LT} and the buckling factor χ_{LT}. The ultimate buckling resistance is obtained by multiplication of the cross-sectional capacity with the buckling factor, Eq. (8). For the sections considered, this cross-sectional capacity is equal to the plastic moment resistance. Note that the partial factor is set to unity.

The relative slenderness λ_{LT} depends on the elastic critical buckling load, Eq. (9).

$$M_{b,Rd} = \chi_{LT} M_{pl} \tag{8}$$

$$\lambda_{LT} = \sqrt{\frac{M_{pl}}{M_{cr}}}. \tag{9}$$

According to the code, buckling curve 'a' should be applied for rolled beams with type 1 connections and a ratio h/b equal to or smaller than 2. IPE160 sections are in this category. IPE500 sections have a ratio h/b larger than 2. The code specifies that curve 'b' should be applied for these sections. Curves 'c' and 'd' should be applied for welded sections.

In Fig. 13 the numerically determined buckling factors of beams with type 1 connections are plotted against the relative slenderness. It is shown that the relation between elastic critical buckling load and ultimate buckling resistance of IPE160 sections
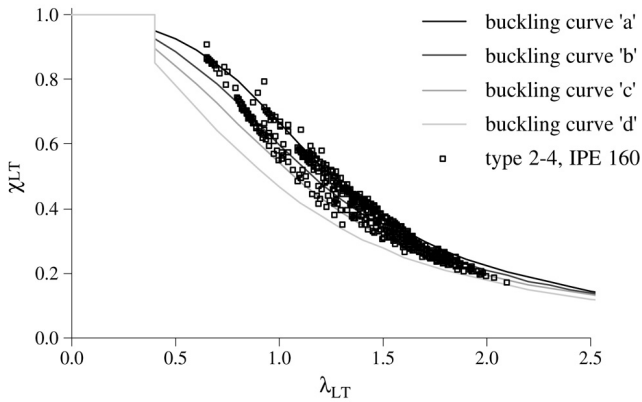
Fig. 14. Buckling curves and simulations of IPE160 beams with type 2–4 connections.
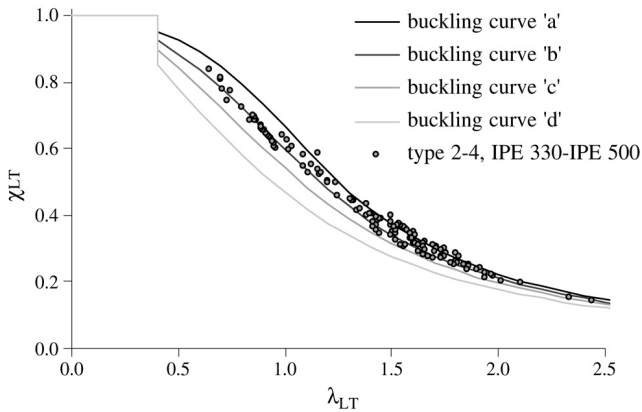

Fig. 15. Buckling curves and simulations of IPE500 beams with type 2–4 connections.

indeed corresponds to buckling curve 'a', and that curve 'b' is a lower border for this relation in the case of IPE500 sections.

Fig. 14 gives the results of numerical simulations of IPE160 beams with type 2–4 connections together with the buckling curves. It is shown that curve 'a' gives for most simulations an unsafe prediction of the ultimate buckling resistance.

Results of numerical simulations of IPE330 and IPE500 sections are given in Fig. 15. The ratio h/b is larger than 2 for these sections, so that curve 'b' should be applied for type 1 connections. Fig. 15 shows that this curve provides in most cases a safe prediction of the ultimate buckling resistance of type 2–4 connections, but not always.

Comparing Figs. 14 and 15 with Fig. 13, it appears that type 2–4 connections give in most cases a lower buckling factor (χ_{LT}) than beams with type 1 connections with the same slenderness.

In the case of type 1 connections, the b/t ratio determines the choice of the appropriate buckling curve (Fig. 13). A correlation between the b/t ratio and the buckling curve appears to be not present in the case of type 2–4 connections. An explanation for this is that in practice, larger h/b ratios occur for larger sections. The cope dimensions relative to the beam depth or span are smaller for such beams with larger sections and consequently the influence of such connections on the ultimate buckling resistance is smaller. Because a maximum value of 65 mm for e_b is used, the same reasoning applies for the dimensions of the parts of the web that are not supported by the short endplate. Thus, although larger sections in general have a larger h/b ratio resulting in a less favourable buckling curve, the influence of the connections is smaller, resulting in a more favourable buckling curve than smaller sections with the same connections.

Based on the numerical simulations, proposals for the appropriate buckling curve are made for beams with type 2–4 connections. Based on the observations given above, the h/b ratio of the section was not taken into account. The choice was based on the influence of the connections on the beam behaviour. The reduction factor α for the elastic critical buckling load (Eq. (2)) was used as the parameter that indicates the influence of the connection.

In the following subsections, for each separate connection type the appropriate buckling curve based on the reduction factor α is determined. To determine the resistance of a beam with type 2–4 connections, the following steps should be carried out:

- The reduction factor α for the critical load should be determined depending on the connection type, using Eqs. (3)–(7);
- The critical load of the beam with type 2–4 connections should be determined by multiplying the reduction factor α with the elastic critical buckling load of the reference beam, with the same dimensions but with type 1 connections (Eq. (1) or similar equations for other load cases);
- The relative slenderness should be determined using the critical load of the beam with type 2–4 connections;
- The appropriate buckling curve should be selected, based on the reduction factor α (following chapters);
- The buckling factor χ_{LT} should be determined with the relative slenderness of the beam considered and the appropriate buckling curve;
- The ultimate buckling resistance should be determined by multiplying the buckling factor χ_{LT} with the cross-sectional capacity.

4.2. Design resistance for beams with partial end plates (type 2)

In Fig. 16 the relation between $\chi_{LT} M_{pl}$ and the numerically determined beam capacity $M_{b,\text{num}}$ is plotted as a function of α_2. The results are given for χ_{LT} values determined with buckling curve 'a'.

In order to obtain safe values for the ultimate buckling resistance, the ratio between $\chi_{LT} M_{pl}$ and $M_{b,\text{num}}$ should be smaller than or equal to one. Fig. 16 shows that this is not the case. Using buckling curve 'a' we thus obtain unsafe values for the design resistance.

In the left-hand graph in Fig. 17, buckling curve 'b' was used to determine the buckling factors χ_{LT} while buckling curve 'c' was used in the right-hand graph.
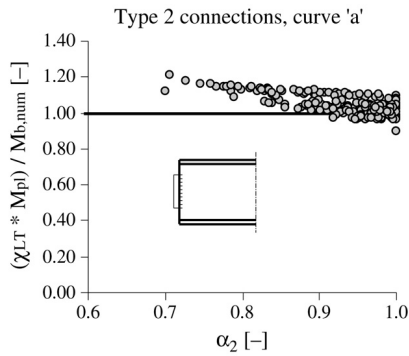
Fig. 16. Ratio design resistance using curve 'a' and numerical resistance as a function of reduction factor α for type 2 connections.
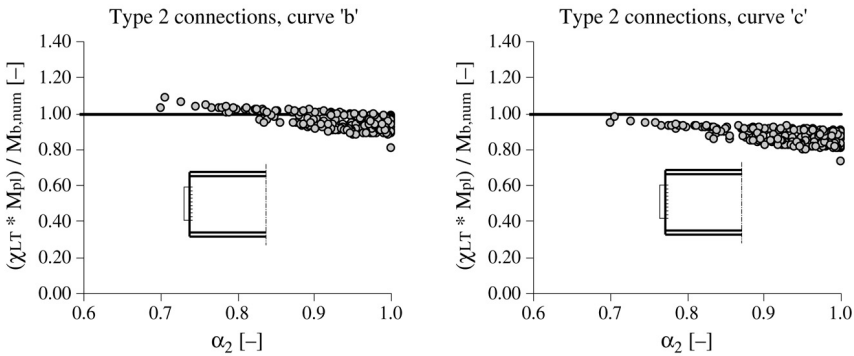

Fig. 17. Ratio design resistance using curve 'b' (left hand) or curve 'c' (right hand) and numerical resistance as a function of reduction factor α for type 2 connections.

It is shown that using curve 'b' results in safe values for the ultimate buckling resistance for large values of α_2, i.e. for small influences of the connection on the critical buckling load. For small values of α_2, curve 'c' can be applied.

The following buckling curve is recommended for beams with type 2 connections:

- For $\alpha_3 \geq 0.85$: buckling curve 'b';
- For $\alpha_3 < 0.85$: buckling curve 'c'.

4.3. Design resistance for beams with copes and long end plates (type 3)

A similar approach is followed for type 3 connections. The left-hand graph in Fig. 18 gives the comparison of the design buckling resistance, using curve 'b' and the numerically determined resistance of beams with type 3 connections. Curve 'c' was applied for the design buckling resistance in the right-hand graph of Fig. 18.

The figure shows that there is no significant correlation between the reduction coefficient α and the appropriate buckling curve in the case of type 3 connections.

Fig. 18. Ratio design resistance using curve 'b' (left hand) or curve 'c' (right hand) and numerical resistance as a function of reduction factor α for type 3 connections.
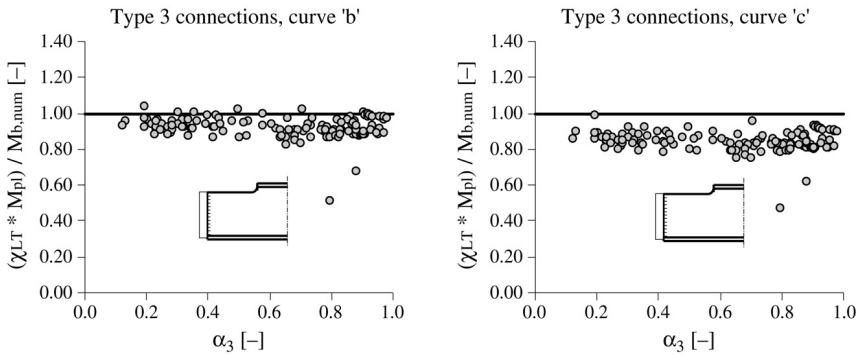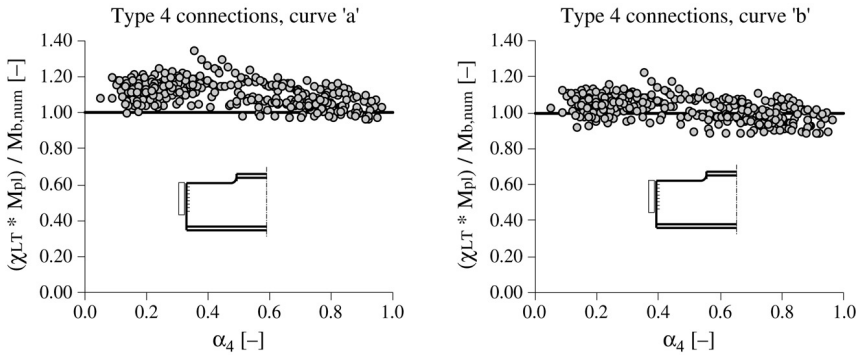

Fig. 19. Ratio design resistance using curve 'a' (left hand) or curve 'b' (right hand) and numerical resistance as a function of reduction factor α for type 4 connections.

It is recommended to apply buckling curve 'b' for beams with type 3 connections, independent of the value of α_3.

4.4. Design resistance for beams with copes and short end plates (type 4)

In Figs. 19 and 20 the results are give for type 4 connections.

Although less apparent than in the case of type 2 connections, there is a correlation between the value of α_4 and the appropriate buckling curve.

The following buckling curve is recommended for beams with type 4 connections:

- For $\alpha_4 \geq 0.85$: buckling curve 'b';
- For $0.45 \leq \alpha_4 < 0.85$: buckling curve 'c';
- For $\alpha_4 < 0.45$: buckling curve 'd'.

The smaller ultimate buckling resistance of coped beams with short end plates is caused by the development of a yield line in the web, causing the whole beam to buckle as
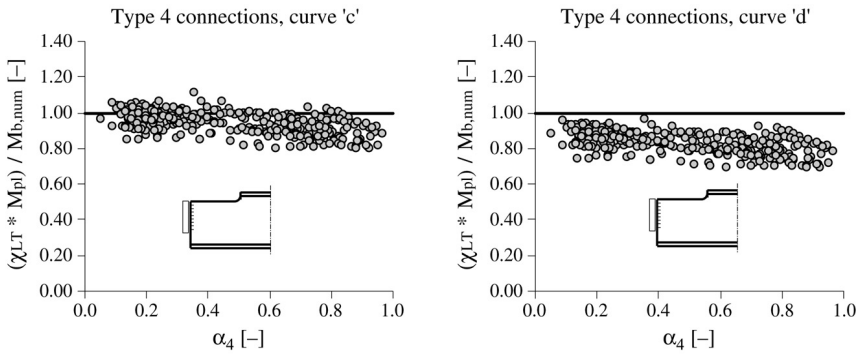
Fig. 20. Ratio design resistance using curve 'c' (left hand) or curve 'd' (right hand) and numerical resistance as a function of reduction factor α for type 4 connections.
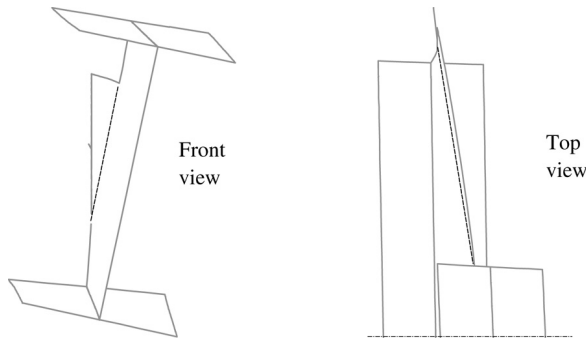

Fig. 21. Lateral–torsional buckling of whole beam initiated by local web buckling.

illustrated in Fig. 21. As a result, the beam does not collapse due to pure lateral–torsional buckling. Other authors provided methods to determine the critical buckling load for the web in the coped section, see e.g. Lam et al. [4]. They recommend to check yielding as well. For an improved treatment of beams with type 4 connections it is recommended to study the yield line mechanism in future research.

4.5. Accuracy of the proposed method

The mean value (μ) and the standard deviation (σ) of the ratio between the design resistance determined with the methods described above and the numerically determined resistance of all simulated beams are given in Table 1.

The methods proposed to determine the elastic critical buckling load and the ultimate buckling resistance are derived with a curve fitting method. Strictly these equations are only applicable within the range of parameters used in the parameter study. It is recommended to develop an analytical method for buckling of coped beams. In addition, it is recommended to investigate whether a better criterion is available to select an appropriate buckling curve than the value of the reduction factor of the elastic critical buckling load.

Table 1
Proposed design method compared to numerical results

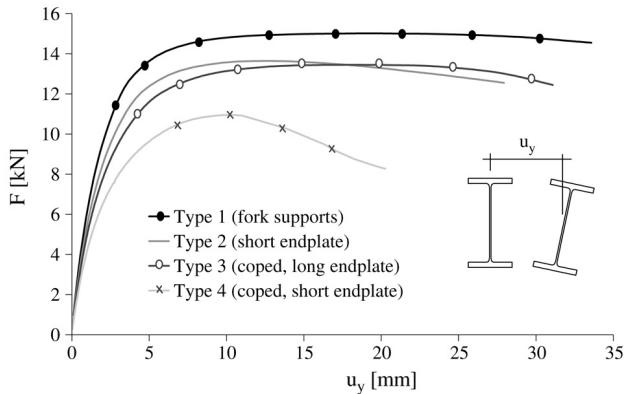|	μ	σ
Type 2 connections	0.95	0.035
Type 3 connections	0.90	0.096
Type 4 connections	0.86	0.11

Fig. 22. Force–lateral displacement diagram for beams with various connections.

5. Post-buckling behaviour

Copes might not only influence the buckling load, but also the maximum deformations and post-buckling behaviour. In order to obtain an idea of the influence of the connection on the post-buckling behaviour, the load–lateral displacement diagrams of beams with five types of connections are shown in Fig. 22. In this figure, the results of numerical simulations of stocky IPE120 beams with a span of 2.5 m ($h/L = 1/20$), loaded by a concentrated load in the center of the upper flange at mid-span are shown.

The post-buckling behaviour for the coped beam with short end plates (type 4) is limited. It should be studied whether these effects are also present for larger spans, longer endplates and smaller cope dimensions.

6. Conclusions and recommendations

Use of short end plates and copes reduces the ultimate buckling resistance. The influence is particularly significant for beams with relatively small span to depth ratios.

As the cope dimensions are relatively larger for beams with smaller depth, the influence of the connection on the ultimate buckling resistance is larger for beams with smaller depths.

Buckling curves 'a' and 'b', given in EN 1993-1-1 for the determination of the ultimate buckling resistance, are in some cases unsafe to apply for beams with copes.

The post-buckling behaviour of coped beams with short end plates is worse than of beams with fork supports.

In this paper simplified equations are given for the determination of the elastic critical buckling load.

Also guidelines are given for the choice of the adequate buckling curve dependent of the end conditions of the beam.

It is recommended not to use stocky beams with large copes in combination with short end plates, as this gives the largest reduction of the ultimate buckling resistance of all studied connections.

Additional research on the following topics is recommended:

- The influence of copes on lateral–torsional buckling of beams loaded by other loads than a uniformly distributed load;
- The influence of cope dimensions on lateral–torsional buckling of beams, connected to the main beam with fin plates or angles;
- Development of an analytical model for yielding of the coped region;
- Development of an analytical model for elastic critical buckling of coped beams;
- Reliability analysis on the influence of variation of dimensions, yield stress and non-straightness on lateral–torsional buckling of coped beams.

References

[1] Maljaars J, Stark JWB, Steenbergen HMGM, Abspoel R. Development and validation of a numerical model for buckling of coped beams. Journal of Constructional Steel Research 2005;61(11):1576–93.

[2] Lindner J, Gietzelt R. Zur Tragfähigkeit ausgeklinkter Träger. Stahlbau 1985.

[3] Cheng JJR, Yura JA, Johnson CP. Lateral buckling of coped steel beams. Journal of Structural Engineering, ASCE 1988;114(1):1–15.

[4] Lam CC, Yam MCH, Iu VP, Cheng JJR. Design for lateral–torsional buckling of coped I-beams. Journal of Constructional Steel Research 2000;54:423–43. Elsevier.

[5] Abspoel R, Stark JWB. Elastic lateral buckling of coped beams. In: Proceedings of eurosteel 1999. Elsevier; 1999.

[6] Abspoel R, Stark JWB. Elastic lateral buckling of coped beams. In: Stability and ductility of steel structures [Proceedings of the 6th international colloquium 1999]. Elsevier; 1999.

[7] Gupta AK. Buckling of coped steel beams. Journal of Structural Engineering, ASCE 1984;110(9):1977–87.

[8] Lindner J. Influence of constructional details on the load carrying capacity of beams. Engineering Structures 1996.

[9] Lindner J. Influence of structural connecting details on the load carrying capacity of beams. In: Internationale Vereinigung für Brückenbau und Hochbau, 13th congres Helsinki. 1988.

[10] Greiner R, Salzgeber G, Ofner R. New lateral–torsional buckling curves κ_{LT}-numerical simulations and design formulae. ECCS TC 8 – Report 30th June 2000.

[11] EN 1993-1-1. Eurocode 3: Design of steel structures — part 1-1: General rules and rules for buildings.

[12] NEN 6771. TGB 1990 Staalconstructies, Stabiliteit. 2000.

[13] Maljaars J. Lateral–torsional buckling of coped girders. Graduation report. The Netherlands: Delft University of Technology; May 2001.